Experiments on the structure and stability of mode 2 internal solitary-like waves

Magda Carr (Mathematical Institute, University of St Andrews, UK)
Peter A Davies (Department of Civil Engineering, University of Dundee, UK)
Ruud Hoebers (Department of Applied Physics, Eindhoven University of Technology, NL)

1 Introduction

Nonlinear internal solitary waves (ISWs) attract interest because many aspects of their behaviour require further theoretical analysis to describe them fully and because they occur (and are important dynamically) in many oceanic contexts (*e.g.* Vlasenko *et al.*, 2005; Apel *et al.*, 2006). The focus of the present study is the generation and development of mode-2 ISWs, a class that has been studied extensively by theoretical and laboratory modellers (*e.g.* Akylas & Grimshaw, 1992; Stamp & Jacka, 1996; Terez & Knio, 1998; Schmidt & Spigel, 2000; Gavrilova & Lyapidevskii, 2009) and for which there are many observational examples in the ocean (*e.g.* Yang *et al.*, 2009; Schroyer *et al.*, 2010). The study has been inspired particularly by recent numerical modelling studies of Salloum *et al* (2012) and Olsthoorn *et al* (2013) in which, *inter alia,* the stability and the tendency to asymmetry of mode-2 waves has been investigated for symmetrical and asymmetrical initial conditions.

2 The experiments

Fig 1 shows a side view of the experimental arrangement; a tank of length 6.4 m, width 0.4 m and rectangular cross section was divided into 2 sections by a vertical gate situated a distance L_G from one end. Within the main part of the tank, a quiescent, 3-layer, stably-stratified fluid system was established by filling sequentially with homogeneous saline layers of density ϱ_1 and ϱ_3 and respective thickness h_1 and h_2 separated by an interfacial layer of thickness h_3 and density $\varrho(z)$, where z is the coordinate in the vertical direction.

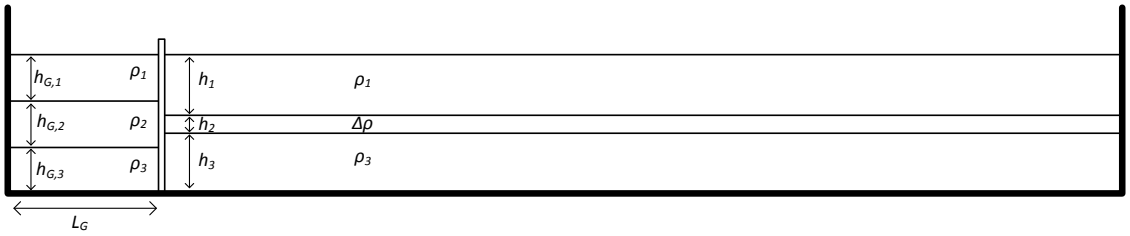

Fig 1. Schematic view of the experimental arrangement –see text for definitions

Behind the gate were layers of density $\varrho_{1,2,3}$ and thicknesses $h_{G,1}$, $h_{G,2}$ and $h_{G,3}$, with ϱ_2 (= $(\varrho_1 + \varrho_3)/2$). The elevation of the central level of the middle layers at both sides of the gate aligned always to be coincident. The total depth was H (=0.4 m) on both sides of the gate. Cases were run in which the mid-plane of the middle layer was located either at mid depth $H/2$ (the so-called 0%-offset condition) or displaced upwards from the mid-depth by a fraction H/n (n = 5, 10, 20) - henceforth delineated respectively as 20%, 10% and 5% offset conditions. For one set of experiments, the conditions replicated exactly those adopted by Olsthoorn *et al* (2013). The experiment was initiated by the vertical removal of the gate and the ISW was recorded by an array of digital video cameras placed along the outside of the main portion of the tank. The fluid in the main tank only was seeded with tracer particles and the *DigiFlow* PIV system was used to process the recorded images. A fixed array of 4 conductivity sensors was programmed to acquire vertical density profiles through the wave as it passed.

3. Results

Fig 2 shows examples of symmetric, stable waves generated for 0% offset cases; such images are directly comparable with those of Salloum *et al* (2012) and Olsthoorn *et al* (2013). The time series shows the characteristic bulge and symmetric core of the dominant mode 2 wave, with two additional mode 2 waves of decreasing amplitude. As the forcing increases (by increasing either $h_{G,2}$ or L_G, or both, for otherwise identical conditions) shear-induced instability within the core results in (i) overturning at the rear of the bulge and (ii) entrainment from the external fluid. Preliminary results indicate the critical dimensionless amplitude for instability is 2.36 ± 7%, in good agreement with the value of 2.75 obtained by Salloum *et al* (2012). The results also show evidence for the occurrence of the so-called PAC-man bulge feature within the parameter range for

which the feature was observed by Salloum *et al* (2012). Comparisons can be made (Table 1) between the lab data and the numerical results of Olsthoorn *et al* (2013) with regard to (i) the amplitudes $a_{1,2,3}$ of 3 successive mode-2 waves and (ii) the distances x1,2,3 travelled by each wave in the reference elapsed time of t = 100s. The comparisons show good agreement.

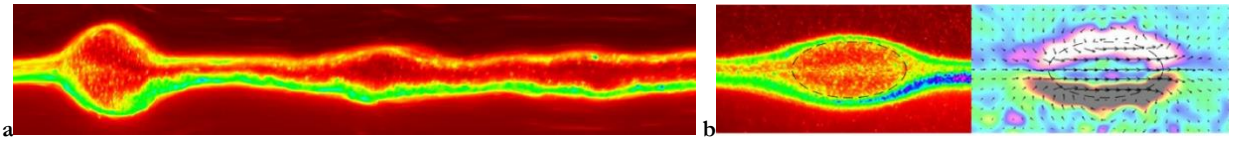

Fig 2. Stable mode-2 wave, 0% offset: (a) typical time series at fixed location, (b) interior core with associated vorticity field

	x_1 (m)	x_2 (m)	x_3 (m)	a_1 (m)	a_2 (m)	a_3 (m)
Numerical	5.40	4.42	3.75	0.0346	0.0213	0.0106
Laboratory	5.40	4.60	4.10	0.0330	0.0170	0.0060

Table1. Comparisons of lab measurements with numerical model results of Olsthoorn *et al* (2013) – see text

For cases of non-zero offset, the results show many of the features described by Olsthoorn *et al* (2013), namely (i) the appearance of mode-1 waves in the tail of the leading mode-2 wave and (ii) top and bottom and fore-aft asymmetry in the shape of the leading mode-2 wave. Increasing the offset value leads to increases in the latter asymmetry and the appearance of localised shear-induced overturning at the rear of the wave (as observed by Olsthoorn *et al*., 2013). As the forcing increases, the vigour of the overturning is seen to increase, with strong top-bottom asymmetry in the overturning (see Fig 3).

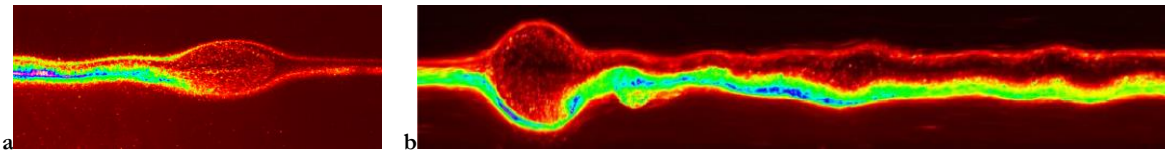

Fig 3. Non-zero offset cases: (a) image containing mode-2 and mode-1 ISWs, (b) time series of unstable mode-2 wave

4 Conclusions

For stable mode-2 waves, the observed flow patterns (and their time development) agree well with relevant numerical model results of Salloum *et al* (2012) and Olsthoorn *et al* (2013). For 0% offset cases, the amplitudes of the dominant and secondary mode-2 waves (and their phase velocities) agree very well with the values obtained numerically by Olsthoorn *et al* (2013) for identical conditions.

The critical amplitude required for instability compares well with the value obtained by Salloum *et al* (2012) for 0% offset cases but the critical amplitude is shown to decreases for increasing offset values. Furthermore, as the offset increases, the top-bottom asymmetry of the manifestation of instability increases.

For unstable 0% offset cases, the strength of the shear-induced billows decreases with elapsed time as more mode-2 waves form in the tail.

References

Akylas,T R & Grimshaw, R H J (1992) Solitary internal waves with oscillatory tails. *J. Fluid Mech.* **242**, 279–298

Apel, J R, Ostrovsky, L A, Stepanyants, Y A & Lynch, J.F (2006). ***Internal Solitons in the Ocean***, Technical Report WHOI-2006-04, Woods Hole Oceanographic Institution, Woods Hole, MA02543, USA.

Gavrilova, N V & Lyapidevskii, V Y (2009). Symmetric solitary waves in a two-layer fluid. *Doklady Physics*, **54**, 11, 508–511.

Olsthoorn, J., Baglaenko, A & Stastna, M., (2013). Analysis of asymmetries in propagating mode-2 waves. *Nonlinear Processes in Geophysics*, 20, 59–69.

Salloum, M, Knio, O M & Brandt, A., (2012) Numerical simulation of mass transport in internal solitary waves, *Physics of Fluids*, 24, 016602.

Schmidt, N P & Spigel, R H (2000) Second mode internal solitary waves I- Integral properties and II – Internal circulation. Proc. 5th Intl Symp. on Stratified Flows (ed. G A Lawrence, R Pieters & N Yonemitsu), 809–820

Stamp, A P & Jacka, M (1996) Deep-water internal solitary waves. *J. Fluid Mech.*, **305**, 347–371.

Terez, D E & Knio, O M (1998) Numerical simulations of large-amplitude internal solitary waves. *J Fluid Mech.*, **362**, 53-82.

Vlasenko, V, Stashchuk, N & Hutter, K (2005). ***Baroclinic Tides: Theoretical Modelling and Observational Evidence***. Cambridge University Press, Cambridge, UK.

Yang, Y J, Feng, Y C, Chang, M-H, Ramp, S R, Kao, C-C & Tang, T-Y (2009), Observations of second baroclinic mode internal solitary waves on the continental slope of the northern South China Sea. *J. Geophys. Res*., **114**, C10003.